

Influence of Large Strain Reverse Loading on Dynamic Strain Localization and Failure of Ductile Metallic Rods

Longhui Zhang^{1*}, David Townsend¹

¹ University of Oxford, Parks Road, Oxford, OX1 3PJ, U.K.

* Presenting Author emails: lh Zhang.mechanics@gmail.com & longhui.zhang@eng.ox.ac.uk

Abstract

A bespoke real time strain control setup is designed to apply the reverse loading directly to the gauge section of ductile metallic rod (304L stainless steel as a model material) up to a maximum strain level of ± 0.16 . The subsequent tensile tests of the reverse loaded specimens are performed from quasi-static to high strain rates of 1000 /s using a bespoke split Hopkinson tension bar. A higher strain reverse loading significantly influences the development of necking instabilities, with smaller strain to necking inception, higher local stress in the necking zone, and higher local strain rate up to failure. An analysis of the local stress-strain relationship indicates that the reverse loaded 304L rod shows good impact energy absorption up to failure, which agrees with the ductile fracture surfaces of the 304L materials with reverse loading.

1. Introduction

The engineering materials in service are inevitably subjected to impact loading. It's important to evaluate the energy absorption of the materials. The mechanical behavior of metallic alloys is influenced by a series of parameters, such as strain rate (and temperature) in the monotonic loading process up to failure. However, the properties of the initial materials in the test would be not the same as those in service. Likewise, the test condition would not meet the service condition. The mechanical property of materials may be weakened by the cycle loading. In the manufacturing process or service, the cycle loading is unavoidable. It is important to study the mechanical response of materials after cycle loading. Tensile test of alloys is associated with necking beyond a maximum load and the strain localization with a decreasing force. Application of materials at high speed deformation requires an understanding of the dynamic strain localization. However, limited effort has been made to monitor and study the dynamic strain localization and the subsequent fracture of materials with reverse loading history in the literature. In the aerospace industry, there is an increasing demand in reducing weight and fuel consumption. The 304L stainless steel with high strength/weight ratio and outstanding resistance to corrosion is important in the jet engine containment application. The understanding of the influence of reverse loading on the subsequent impact resistance and energy absorption is of considerable interest to the engineering and material communities.

2. Results

A bespoke reverse loading setup is built, which is based on the screw-driven Zwick Z50 machine and the Imetrum video extensometer system (Fig. 1A(a-b)). The engineering strain of the 3 mm long gauge section is monitored by Imetrum in real time. This provides feedback to the Zwick machine to apply the strain controlled reverse loading directly to the specimen gauge section at quasi-static of 10^{-2} /s. For the low strain reverse (LSR) loading, when the tensile strain of gauge section reached +0.08, the specimen is unloaded. The unloaded specimen is immediately subjected to reverse compressive loading up to a compressive strain of -0.08, followed by unloading. The engineering stress-strain during this LSR process is shown in Fig. 1A(c). Similarly, the high strain reverse (HSR) loading is applied up to a strain of ± 0.16 . The microstructure of the initial 304L from EBSD is given. With the increase of equivalent plastic strain, the average grain size reduces from 24 μm in the initial 304L to 8 μm in the 304L with HSR loading.

Fig. 1B(a-c) compares the typical local true stress-strain relations of the initial 304L and the 304L with LSR and HSR loading at quasi-static of 10^{-2} /s, medium strain rate of 10^1 /s and high strain rates of about 10^3 /s. The corresponding fracture surfaces at high strain rates are provided, in which a high density of dimples exists (white arrows). The local true stress and true strain at the center of necking are given by $\sigma_{true} = \frac{F}{\pi r^2}$ and $\epsilon_{true} = 2 \ln(\frac{r_0}{r})$. Here, F is the instantaneous acting force, r is the current radius of the minimum cross section of gauge section, r_0 is the initial radius of the gauge section. The change of radius can be obtained from the image analysis, as shown in Fig. 1B(f). The local stress across various strain

rates is amplified in the 304L with reverse loading history, compared to the initial 304L. In the range of the local strain from 0 to 0.30, the local flow stress increases significantly with increasing strain rate. Beyond the local strain of 0.30, the local flow stress values at medium and high strain rates are gradually smaller than that at static loading. The dynamic true strains to failure are lower than that under static condition, which can be observed in both of the initial and reverse loaded 304L. This indicates the flow and failure in the true stress-strain relation show apparent strain rate dependence. Fig. 1B(d) shows the typical local strain rate of the 304L without reverse loading, with LSR and HSR loading, at a comparable nominal strain rate of 900-1100 /s. The true strain rate continues to increase rapidly, due to the strain localization. The local true strain rate reaches a value of one order of magnitude higher than the nominal strain rate. The 304L with HSR loading presents a higher local true strain rate at a given true strain.

Fig. 1B(e) compares the impact energy absorption ($W = \int_0^\epsilon \sigma_{true} d\epsilon_{true}$) of the 304L without reverse loading, with LSR and HSR loading. The initial 304L and the 304L with LSR loading show a similar increase of the strain energy density, with the energy density at failure about 1100 J/m³. The 304L with HSR loading presents a significant increase of the strain energy density at a given true strain. The strain energy density at failure for the 304L with HSR loading is about 1050 J/m³, which is only 5% lower than the initial 304L and the 304L with LSR loading. Although the HSR loading reduces the strain hardening and slightly reduces the true strain to failure, the impact energy absorption of the 304L can still be maintained.

The fracture surfaces of the dynamically failed 304L are examined. The elongated dimples are evenly distributed in the dynamically failed 304L without reverse loading and with LSR loading (Fig. 1B(a-b)),. A high density of dimples exists in the dynamically failed 304L with HSR loading (Fig. 1B(c)), which is attributed to the significant grain size refinement during the reverse loading. Voids can be observed in the fracture surfaces of 304L, regardless of the reverse loading history. This microstructural characterization aims at illustrating that the 304L rods with three different loading conditions present ductile failure mode. This is consistent with the good impact energy absorption of the reverse loaded 304L.

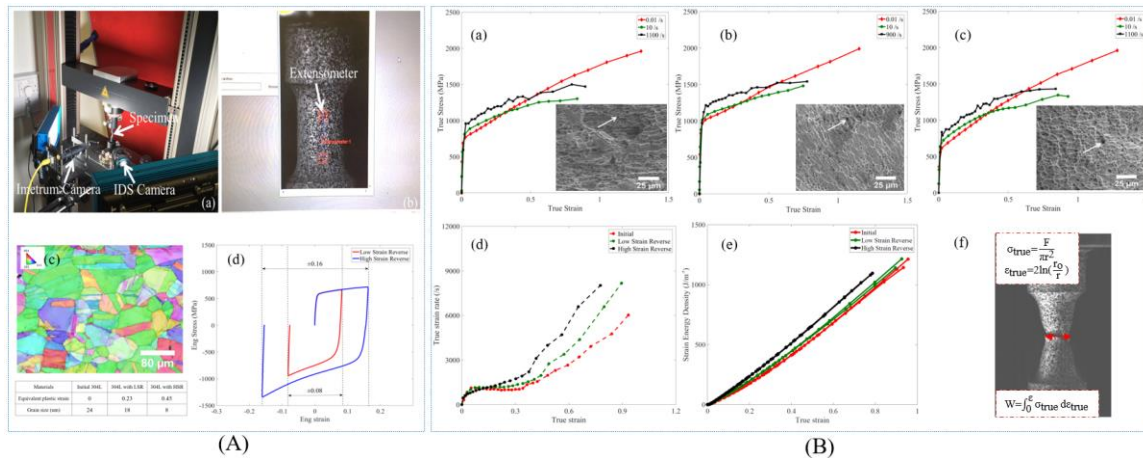


Fig.1 – (A) Reverse loading process and (B) Local responses of the reverse loaded 304L rods

3. Conclusions

This work presents the dynamic strain localization and failure of the 304L and its dependence on the large strain reverse loading history. The large strain reverse loading results in an early necking and the subsequent strain localization during most of the test duration. The 304L materials with reverse loading history show good impact energy absorption up to fracture, which agrees with the microstructural characterizations with ductile failure mode.

Acknowledgements

The authors would like to acknowledge Rolls-Royce plc for their continuing support through the University Technology Centre (UTC) at the University of Oxford.